Multistep Redox Systems, LXIV[1]

DCNQI Anion-Radical Salts with Bisammonium Cations[2]

Siegfried Hünig*[a], Tobias Metzenthin[a], Karl Peters[c], Jost-Ulrich von Schütz[b], and Hans Georg von Schnering[c]

Institut für Organische Chemie der Universität Würzburg[a],
Am Hubland, D-97074 Würzburg, Germany

3. Physikalisches Institut der Universität Stuttgart[b],
Pfaffenwaldring 57, D-70569 Stuttgart, Germany

MPI für Festkörperforschung[c],
Heisenbergstraße 1, D-70506 Stuttgart, Germany

Received November 26, 1997

Keywords: Conducting materials / Radical ions / Crystal structures / Electrochemistry / Dications

Radical-anion salts have been prepared by electrocrystallization from seven 2,3- and 2,5-disubstituted DCNQIs and the quaternary dications (AMM^{2+}) HMED, DMBP, EBP, and EBBT. The black compounds adopt the stoichiometry DCNQI/dication = 3:1. The crystal-structure analysis of two of these radical salts reveal skewed (zigzag, trimerized) stacks of DCNQI molecules separated by sheets of dications. Specific interactions between DCNQI anions and dications are absent. The effect on the stacking of the DCNQI units of the two positive charges in the dications which are held apart at a defined separation is discussed. The salts are shown to be semiconductors with powder conductivities of 10^{-2} to 10^{-5} S cm^{-1}.

N,N′-dicyanoquinone diimines (DCNQIs) have been demonstrated to yield a large variety of highly conducting radical-anion salts with monovalent cations of the stoichiometry $[DCNQI]_2M$ (M = Li, Na, K, NH_4, Rb, Tl, Cu, Ag). In these salts the nitrile groups of the anions are coordinated to the central metal ions forming skewed stacks of the ligands (space group $I4_1/a$ or closely related). This special arrangement of the DCNQI ligands, however, is restricted to 2,5-disubstituted DCNQIs[3] and cannot be obtained with e.g. 2,3-disubstituted DCNQIs.[4]

If ammonium ions are employed instead of monovalent metal ions, DCNQI radical-anion salts of varying stoichiometry are formed with reasonable conductivities (Scheme 1) similar to their TCNQ counterparts.[5]

As far as the crystal structures of these DCNQI salts are known, the anionic ligands are arranged in zigzag stacks which provide one-dimensional conductivity. The ammonium ions are distributed within holes in the crystal lattice, obviously balancing crystal forces with Coulomb attractions. There are no specific interactions to be seen between anions and cations (examples **A**[6], **B**[7], **C**[8]).

We therefore set out to tune the crystal packing of the DCNQI units by employing quaternary dications. In this way, the cations cannot simply be placed in the same way as in examples **A** and **B** since the second positive charge is separated from the first by a defined distance. These dications therefore impose special crystal structures on their DCNQI radical-anion salts according to their geometry. For our experiments we selected the following dications: Hexamethyl-1,2-ethane-diammonium ion (HMED), *N,N′*-dimethyl-4,4′-bipyridinium ion (DMBP), *N,N′*-ethylene-

Scheme 1. DCNQI radical-anion salts **1** with monovalent ammonium cations

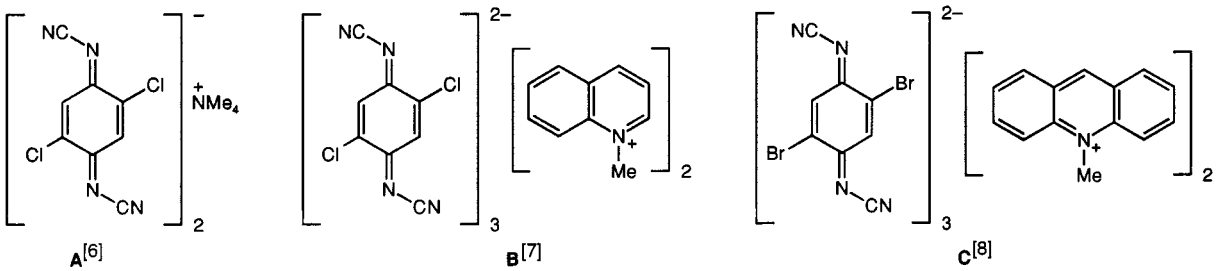

A[6] Monoclinic needles, space group C2/m, σ = 0.2 Scm^{-1}

B[7] Triclinic needles, space group P1, σ = 0.1 Scm^{-1}

C[8] Black cubes

  1434–193X/98/0808–1653 $ 17.50+.50/0

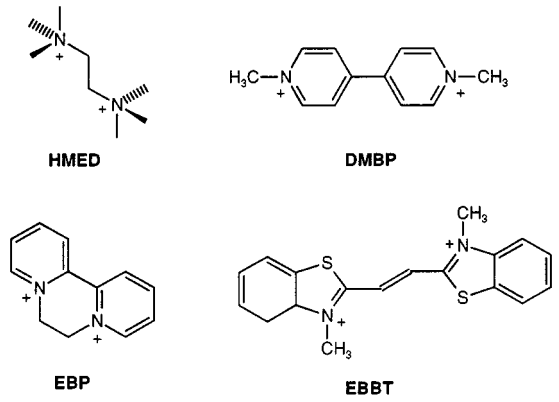

2,2′-bipyridinium ion (EBP),and 2,2′-ethenediylbis(3-methylbenzothiazolium) ion (EBBT).

Only HMED does not offer any π interactions but does allow certain conformational flexibility. In contrast, the three other dications constitute nearly planar π systems in which the distance between the two positive charges increases with EBP < EBBT < DMPP. The reversible reducibility of these three dications[9] does not come into play since the DCNQIs donors employed are too weak for these dicationic acceptors.

Results and Discussion[10]

Earlier experiences have shown that electrocrystallization in acetonitrile can be performed at −20°C if the ammonium ions carried tetrafluoroborate or hexafluorophosphate anions. However, with these highly soluble compounds radical-anion salts were deposited at the platinum electrode only from those DCNQIs which carried at least one halogen substituent. Since the expected crystal structures of the radical salts should not be restricted to the very specific arrangement of 2,5-disubstituted DCNQI metal salts (space group $I4_1/a$)[3], 2,3-disubstituted DCNQIs have also been included (Table 1).

With the other DCNQIs only a blue tint of the cathodic compartment of the H cell was observed. Repetition of these electrolyses in acetonitrile/1,2-dichloroethane mixtures yielded only intractable tarry solids.

The remarkable influence of the nature of the DCNQI substituents cannot be connected to their difference in reduction potentials for several reasons: 1. Electrolysis was performed at constant current and was not potentially controlled. 2. Obviously, the similar volumes of the methyl and bromine substituents are decisive. Only the latter and the even smaller chlorine substituent guarantee solid DCNQI radical-anion salts probably due to their specific polartiy and lower entropic effects (Table 1).

Table 1. Radical-anion salts by electrocrystallization of DCNQIs and bisammonium ions $AMM^{2+}\cdot 2\ X^-$ in acetonitrile at −20°C

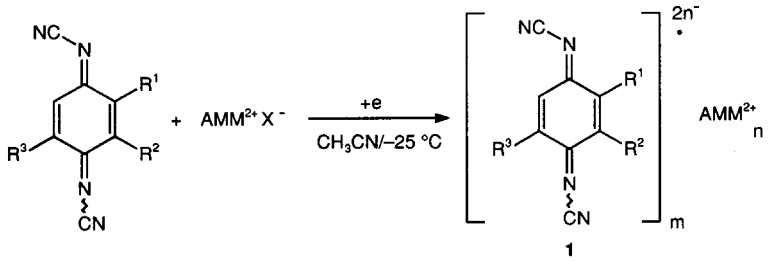

1

Entry	No.	DCNQI R^1	R^2	R^3	AMM^{2+}	*m*:*n*[a]	TS[b]	Yield [%]	m.p.[c] [°C]	σ_P[d] [S cm^{-1}]
1	**1a**	Cl	Cl	H	HMED	8:3	[f]	17	194	2×10^{-5}
2	**1b**	Br	Br	H	HMED	3:1	[f]	4	151	3×10^{-4}
3	**1c**	Cl	H	Cl	HMED	3:1	[f]	56	165	4×10^{-4}
4	**1d**	Br	H	Br	HMED	8:3	[f]	26	169	8×10^{-4}
5	**1a**	Cl	Cl	H	DMBP	3:1	[h]	35	170	3×10^{-3}
6	**1b**	Br	Br	H	DMBP	3:1	[g]	23	175	7×10^{-3}
7	**1c**	Cl	H	Cl	DMBP	3:1	[g]	42	169	7×10^{-4}
8	**1d**	Br	H	Br	DMBP	3:1	[g]	21	290	3×10^{-2}
9	**1e**	Cl	H	CH_3	DMBP	3:1	[g]	45	128	3×10^{-3}
10	**1f**	Br	H	CH_3	DMBP	3:1	[h]	41	128	0.1[e]
11	**1a**	Cl	Cl	H	EBP	3:1	[f]	47	158	3×10^{-2}
12	**1b**	Br	Br	H	EBP	3:1	[g]	50	176	2×10^{-5}
13	**1c**	Cl	H	Cl	EBP	5:2	[h]	45	180	2×10^{-2}
14	**1d**	Br	H	Br	EBP	3:1	[g]	32	183	5×10^{-2}
15	**1e**	Cl	H	CH_3	EBP	3:1	[h]	31	136	0.1[e]
16	**1f**	Br	H	CH_3	EBP	3:1	hl]	26	131	2×10^{-2}
17	**1g**	I	H	CH_3	EBP	3:1	[f]	28	106	7×10^{-5}
18	**1d**	Br	H	Br	EBBT	3:1	[f]	24	96	3×10^{-2}
19	**1f**	Br	H	CH_3	EBBT	8:3	[f]	50	145	1×10^{-2}

[a] Ratio anion/dication from elemental analysis. – [b] Type of solid state. – [c] Differential thermoanalysis. – [d] Powder conductivity. – [e] Single-crystal conductivity. – [f] Amorphous. – [g] Polycrystalline. – [h] Needles.

Table 2. Activation energies ΔE [eV] and factor σ_o [S cm^{-1}] of [**1f**]$_3$/DMP (Figure 1) and [**1e**]$_3$/EBP, two samples (A, B) after 11 weeks (A′, B′) (Figure 2)

Compound	Figure	ΔE [eV]	σ_o [S/cm]
[**1f**]$_3$/DMBP	1	0.14 ± 0.01	28
[**1e**]$_3$/EBP	2A		11
	2B	0.11 ± 0.01	11
	2A′		1.8
	2B′		1.4

Figure 1. Temperature-dependent conductivity of [2-Br,5-Me-DCNQI]$_3$ ([**1f**]$_3$)/DMBP

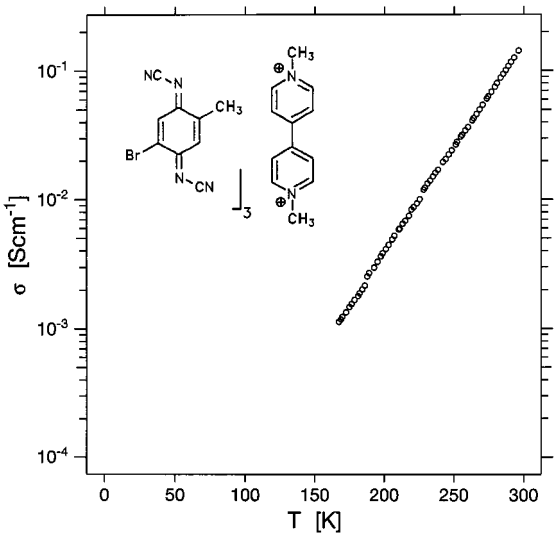

Conductivities of the Radical Salts

Despite of their rather different texture all the products of Table 1 are black solids. This color, together with hardly structured IR spectra, signalize already reasonable conductivities which are found between 10^{-3} and 10^{-2} S cm^{-1}.

As these values are measurements on powdered samples which suffer from contact problems between the grains (percolation) and depend on the pressure applied, single-crystal conductivities larger by at last two orders of magnitude are expected.

Fortunately, in two cases the quality of the crystals was sufficient for single-crystal conductivity measurements (Table 1, entries **10** and **15**: 0.1 S cm^{-1}) and X-ray structure determination.

The temperature-dependend conductivity of both [2-Br,5-Me-DCNQI]$_3$ ([**1f**]$_3$)/DMBP (Figure 1) and [2-Cl,5-Me-DCNQI]$_3$ ([**1e**]$_3$)/EBP (Figure 2) prove these salts to be semiconductors.

The activation energies ΔE and preexponential factor σ_o given in Table 2 could be determined. The respective fits are given in Figure 2 as solid lines.

For ([**1e**]$_3$)/EBP there is a clear degradation observable, the absolute values of σ_o have decreased by a factor of 10. Generally, conductivity results from the product of mobility and number of charge carries (Eq. 1).

$$\sigma(T) = \mu(T)\cdot n(T) = \sigma o\cdot\exp(\Delta E/kT) \quad (1)$$

Figure 2. Temperature-dependent conductivity of [2-Cl,5-Me-DCNQI]$_3$ ([**1e**]$_3$)/EBP; two samples (A, B) after 11 weeks (A′, B′)

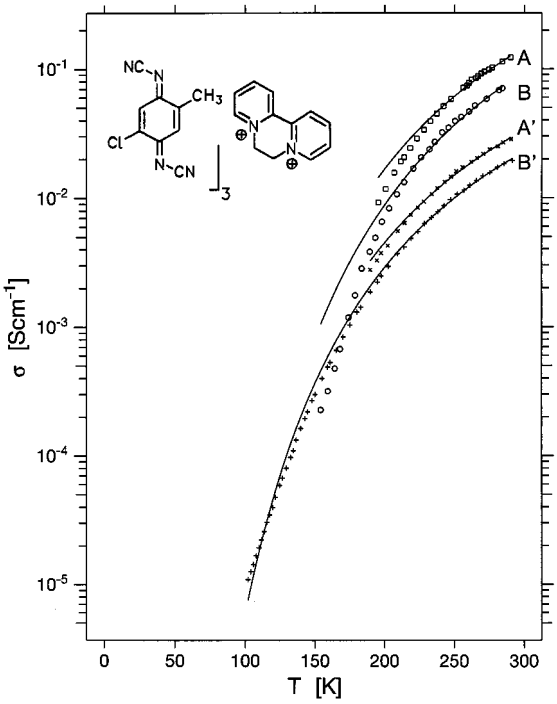

For the separation of charge carries activation we have performed ESR experiment on [**1e**]$_3$/EBP given in Figure 3. The product $\chi\cdot T$ is plotted versus T, a measure for the number of spins present. The initial slope at high temperature can be fitted by an activation energy of about 0.06 eV rather close to that of $\sigma(T)$, representing a lower limit for the band gap.

Figure 3. Temperature-dependent susceptibility of [2-Cl,5-Me-DCNQI]$_3$([**1e**]$_3$)/DMBP (o) after 11 weeks (+)

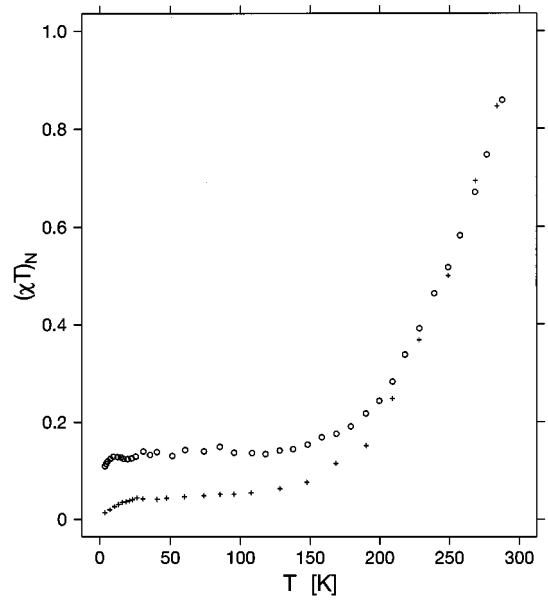

There exists a rather large concentration of residual spins which give rise to the flat $\chi\cdot T$ response below 150 K.

The idea of degradation mentioned above is supported by the ESR on the "aged" crystals: The number of residual spins has increased by a factor of 3. As these spins may act as scattering centres for the conduction electrons, the increase in $\chi \cdot T$ is in agreement with the decrease in the absolute conductivity.

Crystal Structures

[2-Br,5-Me-DCNQI]$_3$ ([**1f**]$_3$)/DMBP: The structure determination of this radical salt turned out to be rather difficult. The DCNQI units are disordered with respect to their bromine and methyl substituents. The bromine substituent is a strong dispersing entity and the methyl substituent a weak dispersing entity, making evaluation of the electron density at the important 2- and 5-positions of the DCNQI moiety insufficient for a full structural determination. Besides, the crystals belong to the acentric space group *C*2, thereby reducing again the experimental data available for the evaluation of the positions of the relevant atoms. Therefore the structure could only be refined with isotropic temperature coefficients to $R = 15.6\%$. This situation allows only a qualitative discussion of the structure of the crystal lattice.

A view onto the *a*,*c* plane of the crystal shows separate stacks of anions and cations (Figure 4). The DCNQI molecules are positioned along their π faces in skewed stacks producing a "ring-over-bond" arrangement[11] which is favorable for electron transport. This occurs, however, along curved lines (Figure 6) and not in straight stacks as with DCNQI metal salts[3]. In contrast, the dications of DMBP are arranged side-on in monomolecular sheets which separate the anionic stacks from each other. A view onto the *a*,*b* plane (Figure 5) demonstrates the disorder within the DCNQI stacks where even the N−CN group (always anti-configuration) point in different directions. Altogether one finds three kinds of disordered DCNQI units producing six differently oriented anions within the unit cell.

Figure 4. Crystal structure of [2-Br,5-Me-DCNQI]$_3$ ([**1f**]$_3$)/DMBP; view onto the *a*,*c* plane (along [0 −1 0])

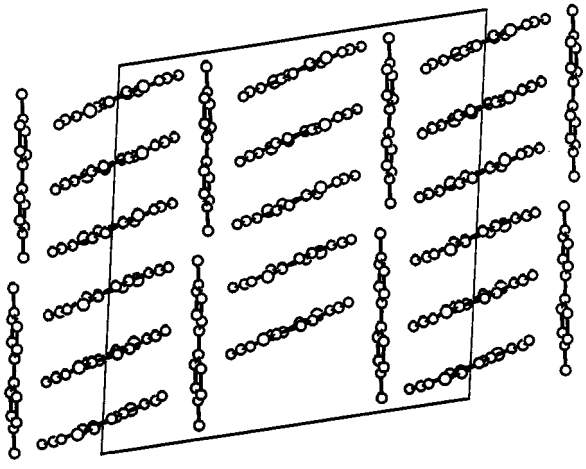

Interestingly, the corresponding TCNQ/DMBP salt occurs with the same stoichiometry (3:1) but differs in its crystal structure.[12] [TCNQ]$_3$/DMBP prefers to adopt the centrosymmetric space group *P*1̄ with only one dication per unit cell. The acceptor stacks consist of skewed trimerized TCNQ units with the typical ring-over-bond pattern (Figure 7). Furthermore, the planes of acceptors and donors are found *not* parallel but perpendicular to one another, similar to the situation in [2-Br,5-Me-DCNQI]$_3$ ([**1f**]$_3$)/DMBP (Figure 4).

Figure 5. Crystal structure of [2-Br,5-Me-DCNQI]$_3$ ([**1f**]$_3$)/DMBP; view onto the *a*,*b* plane (along [0 0 −1])

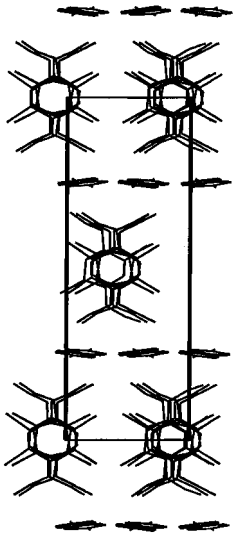

Figure 6. Crystal structure of [2-Br,5-Me-DCNQI]$_3$ ([**1f**]$_3$)/DMBP; vertical view of the central DCNQI stack of Figure 5

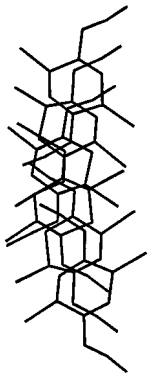

Figure 7. Crystal structure of [TCNQ]$_3$/DMBP; space group *P*1̄[14], view onto the *b*,*c* plane (along [−1 0 0])

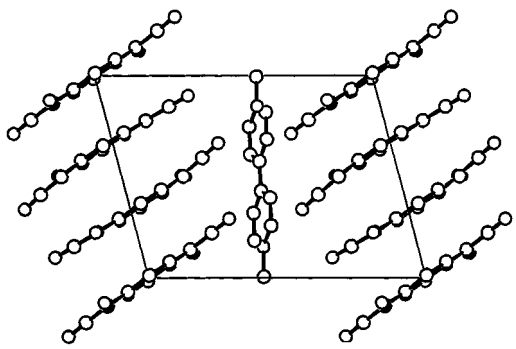

[2-Cl,5-Me-DCNQI]$_3$ ([**1e**]$_3$)/FBP: This compound adopts the triclinic space group *P*1. The large unit cell and the low symmetry of the lattice mean that it was not possible to reduce *R* to < 9%. Therefore only the general structure of the radical salt will be discussed here.

A view along the *a* axis reveals the separate stacking of anions and cations where the latter are again positioned nearly perpendicular to the acceptor stacks (Figure 8). The DCNQI stacks show statistical disorder of the DCNQI units with regard to their chloride and methyl substituents in positions 2 and 5, respectively. Two different types of acceptor stacks were found (Figure 9). Both stacks run parallel to the *a* axis, one through the centre of inversion, the other through the origin of the unit cell.

Figure 8. Crystal structure of [2-Cl,5-Me-DCNQI]$_3$ ([**1e**]$_3$)/EBP; space group *P*1; view along the *a* axis [−1 0 0]

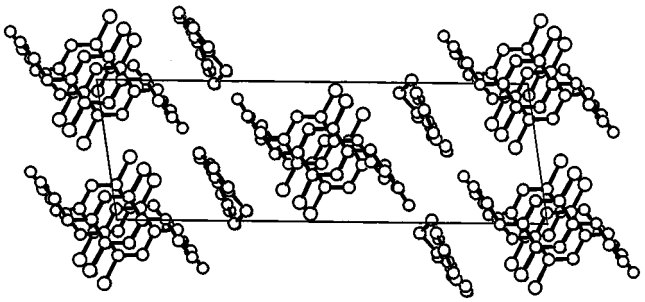

Figure 9. Crystal structure of [2-Cl,5-Me-DCNQI]$_3$ ([**1e**]$_3$)/EBP; space group *P*1 ; view along the *c* axis [0 0 −1]

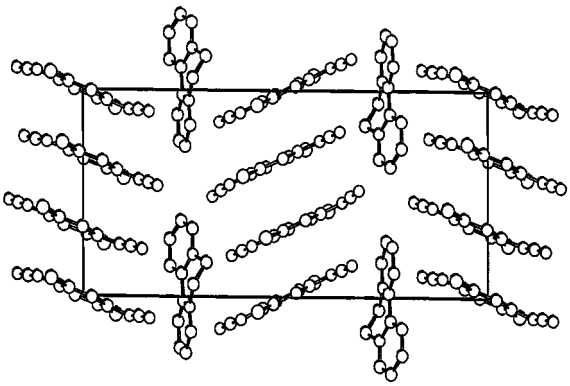

Both stacks contain skewed trimeric units of DCNQI with a rather unexpected pattern (Figure 10). The ring of the first molecule is placed over the quinoid bond of the next, whereas in this molecule the exocyclic double bond is positioned over the ring of the lowest one. In this way, each molecule of the stack contacts one neighbor by a ring-over-bond arrangement and the other by a ring-over-ring approach.

The structure of [2-Cl,5-Me-DCNQI]$_3$ ([**1e**]$_3$)/EBP cannot be compared with the corresponding (TCNQ)$_2$/EBP due to its different stoichiometry, although the same space group *P*1 is found (Figure 11).[13] The low symmetry of the lattice allows various positions for its constituents. The crystals contain only one type of TCNQ stack, however, composed from two types of dimers (AA′, BB′) in a zigzag

Figure 10. Crystal structure of [2-Cl,5-Me-DCNQI]$_3$ ([**1e**]$_3$)/EBP; space group *P*1; packing pattern of the central DCNQI stacks

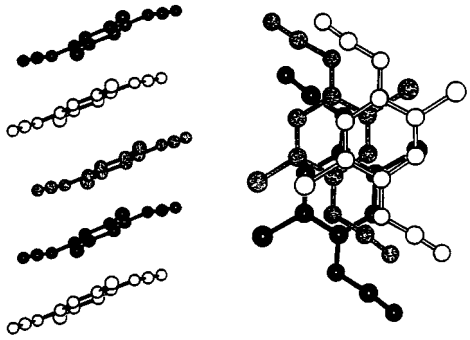

fashion. As with the DCNQI salt only one crystallographic ordering of the dications is found but in a long-distance face-to-face arrangement close to that of the anions rather than a perpendicular head-to-tail organization (Figures 8 and 9).

Figure 11. Crystal structure of [TCNQ]$_2$/EBP;[13] space group *P*1; view onto the *b*,*c* plane

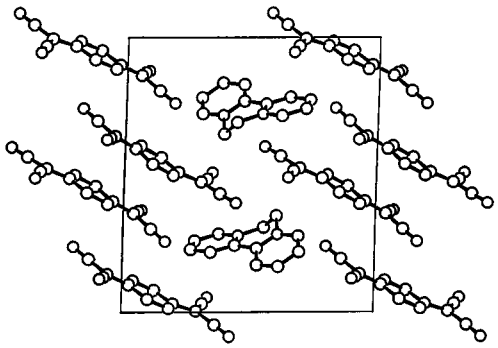

Conclusions

From a variety of 2,3- and 2,5-disubstituted DCNQIs and the dications HMED, DMBP, EBP, and EBBP, radical-anion salts were obtained by electrocrystallization. The black color, the flat IR-spectra and powder conductivities of 10^{-1} to 10^{-3} S cm^{-1} are consistent with crystal lattices with segregated stacks. This structure could be verified only for compounds [2-Br,5-Me-DCNQI]$_3$ ([**1f**]$_3$)/DMBP and [2-Cl,5-Me-DCNQI]$_3$ ([**1e**]$_3$)/EBP. In both cases no specific interactions between anions and cations were observed which would allow the design of specific crystal lattices as was the case with the DCNQI metal salts. In contrast to their salts with monovalent cations[3], the 2,5-disubstituted DCNQIs are therefore not unique. Salts from 2,3-disubstituted DCNQIs and organic dications exhibit the same conductivities. Since most of the radical salts investigated prefer to adopt a 3:1 stoichiometry, analogous crystal structures can be expected for all radical salts with the dications DMBP and EBP. The trimeric or tetrameric nature of the acceptor stacks causes activated conductivity connected with the properties of a semiconductor. This arrangement may be caused by the "twinned" Coulomb potentials of the dicat-

ions which provide alternating intra- and intermolecular separations for the positive charges.

The rather puzzling observation that despite thorough experimentation only the asymmetric substituent combinations (Cl/Me; Br/Me) and not symmetrical ones (Cl/Cl; Br/Br) allowed the growth of single crystals should be mentioned. The resulting dipole moment of those DCNQIs may possibly better accommodate the inhomogenous electrical field provided by the dications allowing the building of more stable crystals.

Although the crystal lattice of [2-Br,5-Me-DCNQI]$_3$([**1f**]$_3$)/DMBP with its sheets of conducting anions and layers of insulating cations (Figure 4) resembles those of superconducting BEDT salts[14], no transition to superconductivity is observed down to ca. 2 K. Such a transition would require equal separations within the DCNQI stacks. However, even BEDT salts which fulfill these requirements do not necessarily demonstrate superconductivity.[15]

Financial support by *Fonds der Chemischen Industrie* and *Studienstiftung des Deutschen Volkes* (T. M.) as well as the donation of valuable chemicals by the *BASF AG*, Ludwigshafen/Rhein, is gratefully acknowledged. We thank *U. Langohr* and *S. Söderholm* for providing the conductivity and ESR data.

Experimental Section

General: IR: Perkin Elmer 1420. − Starting materials: *N,N,N′,N′,N′*-Hexamethyl-1,2-ethanediammonium bis(hexafluorophosphate) (HMED[PF_6]$_2$) by reaction of the diiodide[16] with excess of NH_4PF_6 in water. − 1,1′-Dimethyl-4,4′-bipyridinediylium bis(hexafluorophosphate) (DMBP[PF_6]$_2$) by reaction of the diiodide[17] with excess of NH_4PF_6 in water. − 6,7-Dihydro-dipyrido[1,2-*a*;2′,1′-*c*]pyrazinediylium bis(tetrafluoroborate) [EBP(BF_4)$_2$] by reaction of the dibromide[18] with $NaBF_4$ in water. − 2,2′-Ethenediylbis(3-methylbenzothiazolium) bis(tetrafluoroborate) [(EBBT)(BF_4)$_2$][19]. − *N,N′*-Dicyano-2-X-3-Y- or -2-X-5-Y-1,4-benzoquinone diimines: X = Cl, 3-Y = Cl;[4] X = Cl, 5-Y = Cl;[22] X = Br, 3-Y = Br;[4] X = Br, 5-Y = Br;[20] X = Cl, 5-Y = Me;[20] X = Br, 5-Y = Me;[21] X = I, 5-Y = Me.[21]

Electrocrystallization: Three-compartment cells (C3) or two-compartment cells with enlarged cathodic part (C2). Cathodes: Pt rods (3−4 mm, diameter 1 mm). A solution of the DCNQI and excess dicationic salt (cf. Table 1) were dissolved in acetonitrile (60−80 ml). The solution was degassed sonically and filtered through a cotton pad into the oven-dried cell. This solution was saturated with nitrogen and cooled to the appropriate temperature. After electrolysis for 1−3 weeks the black precipitate was collected in a funnel, washed with acetonitrile, and dried. For melting points and conductivities see Table 1. The stoichiometry of the products was calculated from elemental analyses.

2,3-Dichloro-N,N′-dicyano-1,4-benzoquinonediimine (**1a**)/HMED (8:3): **1a** (56 mg, 250 μmol), HMED(PF_6)$_2$ (327 mg, 750 μmol), C2, −18°C, 10 μA (0.1 mA/cm^2), 4 d; black amorphous solid (12 mg, 17%). − IR (KBr): ν = 3005 cm^{-1}, 2105 (C≡N), 1550, 1480, 1350. − $C_{88}H_{82}Cl_{16}N_{38}$ (2239.1): calcd. C 47.20, H 3.69, N 23,77; found C 47.03, H 4.09, N 23.52.

2,3-Dibromo-N,N′-dicyano-1,4-benzoquinonediimine (**1b**)/HMED (3:1): **1b** (80 mg, 255 μmol), HMED(PF_6)$_2$ (327 mg, 750 μmol), C2, −29°C, 10 μA (0.08 mA/cm^2), 19 d; hard amorphous solid (11 mg, 12%). − IR (KBr): ν = 3005 cm^{-1}, 2100 (C≡N), 1545, 1480, 1350. − $C_{32}H_{28}Br_6N_{14}$ (1088.1): calcd. C 35.32, H 2.59, N 18.02; found C 35.33, H 2.50, N 17.94.

2,5-Dichloro-N,N′-dicyano-1,4-benzoquinonediimine (**1c**)/HMED (3:1): **1c** (56 mg, 250 μmol), HMED(PF_6)$_2$ (218 mg, 500 μmol), C2, −18°C, 10 μA (0.08 mA/cm^2), 19 d; hard amorphous solid (38 mg, 56%). − IR (KBr): ν = 2110 (C≡N) cm^{-1}, 1560. − $C_{32}H_{28}Cl_6N_{14}$ (821.4): calcd. C 46.79, H 3.44, N 23.87; found C 46.89, H 3.66, N 23.29.

2,5-Dibromo-N,N′-dicyano-1,4-benzoquinonediimine (**1d**)/HMED (8:3): **1d** (78 mg, 250 μmol), HMED(PF_6)$_2$ (327 mg, 750 μmol), C3, −18°C, 10 μA (0.08 mA/cm^2), 6 d; amorphous solid (22 mg, 24%). − IR (KBr): ν = 2110 (C≡N) cm^{-1}, 1560. − $C_{88}H_{82}Br_{16}N_{38}$ (2950.3): calcd. C 35.83, H 2.80, N 18.04; found C 35.95, H 2.85, N 18.23.

2,3-Dichloro-N,N′-dicyano-1,4-benzoquinonediimine (**1a**)/DMBP (3:1): **1a** (56 mg, 250 μmol), DMBP(PF_3)$_2$ (375 mg, 750 μmol), C3, −18°C, 10 μA (0.08 mA/cm^2), 8 d; black needles (25 mg, 35%). − IR (KBr): ν = 2100 cm^{-1} (C≡N). − $C_{36}H_{20}Cl_6N_{14}$ (861.4): calcd. C 50.20, H 2.34, N 22.77; found C 50.36, H 2.09, N 22.56.

2,3-Dibromo-N,N′-dicyano-1,4-benzoquinonediimine (**1b**)/DMBP (3:1): **1b** (79 mg, 250 μmol), DMBP(PF_6)$_2$ (357 mg, 759 μmol), C3, 0°C, 5 μA (0.06 mA/cm^2), 10 d; black crystals (22 mg, 23%). − IR (KBr): ν = 2120 cm^{-1} (C≡N). − $C_{36}H_{20}Br_6N_{14}$ (1128.05): calcd. C 38.33, H 1.79, N 17.38; found C 38.09, H 1.56, N 17.10.

2,5-Dichloro-N,N′-dicyano-1,4-benzoquinonediimine (**1c**)/DMBP (3:1): **1c** (56 mg, 250 μmol), DMBP(PF_6)$_2$ (357 mg, 750 μmol), C3, −20°C, 5μA (0.05 mA/cm^2), 17 d; black solid (30 mg, 42%). − IR (KBr): ν = 2100 cm^{-1} (C≡N). − $C_{36}H_{20}Cl_6N_{14}$ (861.4): calcd. C 50.20, H 2.34, N 22.77; found C 50.14, H 2.31, N 22.53.

2,5-Dibromo-N,N′-dicyano-1,4-benzoqujinonediimine (**1d**)/DMBP (3:1): **1d** (78 mg, 250 μmol), DMBP(PF_6)$_2$ (357 mg, 750 μmol), C3, −18°C, 10 μA, (0.08 mA/cm^2), 6 d; polycrystalline solid (20 mg, 21%). − IR (KBr): ν = 2100 cm^{-1} (C≡N), 1550. − $C_{36}H_{20}Br_6N_{14}$ (1128.05): calcd. C 38.33, H 1.79, N 17.38; found C 38.05, H 1.76, N 17.07.

2-Chloro-N,N′-dicyano-5-methyl-1,4-benzoquinonediimine (**1e**)/DMBP (3:1): **1e** (51 mg, 250 μmol), DMBP(PF_6)$_2$ (357 mg, 750 μmol), C3, −18°C, 10 μA (0.08 mA/cm^2), 10 d; black solid (30 mg, 40%). − IR (KBr): ν = 2100 cm^{-1} (C≡N). − $C_{30}H_{29}Cl_3N_{14}$ (800.1): calcd. C 58.55, H 3.65, N 24.51; found C 58.39, H 3.40, N 24.45.

2-Bromo-N,N′-dicyano-5-methyl-1,4-benzoquinonediimine (**1f**)/DMBP (3:1): **1f** (62 mg, 250 μmol), DMBP(PF_6)$_2$ (357 mg, 750 μmol), C3, −20°C, 5 μA (0.04 mA/cm^2), 4 d; black needles (32 mg, 41%). − IR (KBr): ν = 2100 cm^{-1}. − $C_{39}H_{29}Br_3N_{14}$ (933.5): calcd. C 50.18, H 3.13, N 21.01; found C 50.06, H 2.99, N 20.75.

2,3-Dichloro-N,N′-dicyano-1,4-benzoquinonediimine (**1a**)/EBP (3:1): **1a** (68 mg, 303 μmol), EBP(BF_4)$_2$ (340 mg, 950 μmol), C3, −18°C, 10 μA (0.09 mA/cm^2), 9 d; black solid (41 mg, 47%). − IR (KBr): ν = 2100 cm^{-1} (C≡N), 1600, 1550, 1480, 1350. − $C_{36}H_{18}Cl_6N_{14}$ (859.4): calcd. C 50.32, H 2.11, N 22.82; found C 50.46, H2.36, N 23.16.

2,3-Dibromo-N,N′-dicyano-1,4-benzoquinonediimine (**1b**)/EBP (3:1): **1b** (79 mg, 252 μmol), EBP(BF_4)$_2$ (268 mg, 750 μmol), C3, −20°C, 20 μA (0.15 mA/cm^2), 15 d; microcrystalline powder (47 mg, 50%). − IR (KBr): ν = 2100 cm^{-1} (C≡N), 1550, 1480. − $C_{36}H_{18}Br_6N_{14}$ (1126.0): calcd. C 38.40, H 1.61, N 17.41; found C 38.46, H 1.95, N 17.20.

2,5-Dichloro-N,N′-dicyano-1,4-benzoquinonediimine (**1c**)/EBP (5:2): **1c** (68 mg, 300 μmol), EBP(BF_4)$_2$ (347 mg, 970 μmol), C3,

Table 3. X-ray data[22]

Compound	[2,5-Br,Me-DCNQI]$_3$/DMBP	[2,5-Cl,Me-DCNQI]$_3$/EBP
empirical formula	$C_{39}H_{29}Br_3N_{14}$	$C_{39}H_{27}Cl_3N_{14}$
molecular mass	933.47	798.10
a [pm]	2210.6(7)	1051.8(3)
b [pm]	781.4(4)	2278.8(6)
c [pm]	2323.0(8)	753.5(2)
α [°]	90	98.94(2)
β [°]	100.81(3)	95.80(2)
γ [°]	90	88.26(2)
V [pm^3]	$3797(3)\times10^6$	$1774.6(8)\times10^6$
Z	4	2
d(calcd.) [g cm^{-3}]	1.633	1.493
crystal system	monoclinic	triclinic
space group	*C*2	*P*1
diffractometer	STOE-Stadi 4	Siemens R3m/V
radiation	Mo-K_α	Mo-K_α
monochromator	graphite	graphite
crystal size [mm]	0.3 × 0.65 × 0.2	0.35 × 0.75 × 0.2
data-collection mode	θ/θ scan	Wyckoff-scan
θ range [°]	1.75−25.0	1.75−27.5
recip. latt. segment	$h = 0 \rightarrow 26$ $k = 0 \rightarrow 9$ $l = -27 \rightarrow 27$	$h = -13 \rightarrow 13$ $k = -29 \rightarrow 29$ $l = 0 \rightarrow 9$
no. refl. measd.	7203	8202
no. unique refl.	6665	8202
no. refl. $F > 3\,\sigma(F)$	2778	5767
μ [mm^{-1}]	3.21	0.31
abs. correction	geometrical	empirical
solution by	direct-phase determination	
method of refinement	full-matrix least-squares; hydrogen positions: riding model with fixed isotropic *U*	
data-to-parameter ratio	16.55	11.90
R, R_w	0.156, 0.104	0.111, 0.094
weighting scheme	$w = 1/\sigma^2(F)$	
largest difference peak	3.60 e A^{-3}	0.55 e A^{-3}
largest difference hole	4.42 e A^{-3}	0.54 e A^{-3}
program used	Siemens SHELXTL PLUS	

−18°C, 10 μA (0.08 mA/cm^2), 24 d; black needles (33 mg, 37%). − IR (KBr): ν = 2110 cm^{-1} (C≡N). − $C_{64}H_{34}Cl_{10}N_{24}$ (1493.7): calcd. C 51.46, H 2.29, N 22.51; found C 51.15, H 2.22, N 22.21.

2,5-Dibromo-N,N′-dicyano-1,4-benzoquinonediimine (**1d**)/EBP (3:1): **1d** (79 mg, 252 μmol), EBP(BF$_4$)$_2$ (289 mg, 807 μmol), C3, −18°C, 10 μA (0.08 mA/cm^2), 7 d; black solid (30 mg, 32%). − IR (KBr): ν = 2105 cm^{-1} (C≡N). − $C_{36}H_{18}Br_6N_{14}$ (1126.0): calcd. C 38.40, H 1.61, N 17.41; found C 38.58, H 1.52, N 17.35.

2-Chloro-N,N′-dicyano-5-methyl-1,4-benzoquinonediimine (**1e**)/EBP (3:1): **1e** (51 mg, 250 μmol), EBP(BF$_4$)$_2$ (289 mg, 807 μmol), C3, −18°C, 10 μA (0.08 mA/cm^2), 10 d; black needles (3 mm; 20 mg, 31%). − IR (KBr): ν = 2110 cm^{-1} (C≡N). − $C_{39}H_{27}Cl_3N_{14}$ (798.10): calcd. C 58.69, H 3.41, N 24.57; found C 58.66, H 3.17, N 24.74.

2-Bromo-N,N′-dicyano-5-methyl-1,4-benzoquinonediimine (**1f**)/EBP (3:1): **1f** (62 mg, 250 μmol), EBP(BF$_4$)$_2$ (289 mg, 807 μmol), C3, −18°C, 10 μA (0.08 mA/cm^2), 15 d; black needles (20 mg, 26%). − IR (KBr): ν = 2110 cm^{-1} (C≡N). − $C_{39}H_{27}Br_3N_{14}$ (931.4): calcd. C 50.29, H 2.92, N 21.05; found C 50.43, H 2.88, N 20.87.

N,N′-Dicyano-2-iodo-5-methyl-1,4-benzoquinonediimine (**1g**)/EBP (3:1): **1g** (74 mg, 250 μmol), EBP(BF$_4$)$_2$ (347 mg, 970 μmol), C3, −18°C, 10 μA (0.08 mA/cm^2), 8 d; black amorphous solid (25 mg, 28%). − IR (KBr): ν = 2110 cm^{-1} (C≡N). − $C_{39}H_{27}I_3N_{14}$ (1072.4): calcd. C 43.68, H 2.54, N 18.29; found C 43.57, H 2.46, N 18.00.

2,5-Dibromo-N,N′-dicyano-1,4-benzoquinonediimine (**1d**)/EBBT (8:3): **1d** (79 mg, 250 μmol), EBBT(BF$_4$)$_2$ (373 mg, 750 μmol), C3, −18°C, 10 μA (0.08 mA/cm^2), 6 d; black crystals (26 mg, 24%). − IR (KBr): ν = 2110 cm^{-1} (C≡N). − $C_{118}H_{64}Br_{16}N_6S_6$ (3484.8): calcd. C 40.67, H 1.85, N 15.27; found C 40.33, H 1.95, N 15.35.

2-Bromo-N,N′-dicyano-5-methyl-1,4-benzoquinonediimine (**1f**)/EBBT (3:1): **1f** (62 mg, 250 μmol), EBBT(BF$_4$)$_2$ (373 mg, 750 μmol), C2, −18°C, 10 μA (0.08 mA/cm^2), 26 d; black solid (45 mg, 50%). − IR (KBr): ν = 2110 cm^{-1} (C≡N). − $C_{45}H_{31}Br_3N_{14}S_2$ (1071.7): calcd. C 50.43, H 2.92, N 18.30; found C 50.63, H 2.97, N 18.56.

[1] Part LXIII: S. Hünig, R.. Bau, M. Kemmer, H. Meixner, T. Metzenthin, K. Peters, K. Sinzger, J. Gulbis, *Eur. J. Org. Chem.* **1988**, 335-348.
[2] Taken from the Ph.D.Thesis of T. Metzenthin, University of Würzburg, **1991**; cf. also ref.[10].
[3] Review: S. Hünig, *J. Mater. Chem.***1995**, *5*, 1469−1479.
[4] P. Erk, S. Hünig, G. Klebe, T. Metzenthin, H. P. Werner, J.-U. von Schütz, *Liebigs Ann.* **1997**, 1235−1243.
[5] J. H. Perlstein, *Angew. Chem.* **1977**, *89*, 534−549; *Angew. Chem. Int. Ed. Engl.* **1977**, *16*, 519−534.
[6] H.-P. Werner, J.-U. von Schütz, H. C. Wolf, R. K. Kremer, M. Gehrke, A. Aumüller, P. Erk, S. Hünig, *Solid State Commun.* **1989**, *69*, 1127−1130.
[7] S. Hünig, P. Erk, *Adv. Mater.* **1991**, *3*, 225−236.
[8] A. Aumüller, Ph. D. Thesis, University of Würzburg, **1995**.
[9] Cf. review: S. Hünig, H. Berneth, *Top. Curr. Chem.* **1980**, *92*, 1−44.

[10] Preliminary publication: S. Hünig, T. Metzenthin, U. Langohr, J. U. von Schütz, S. Söderholm, H. C. Wolf, K. Peters, H. G. von Schnering, *Synth. Met.* **1991**, *42/1+2*, 1819−1822.
[11] For the effects of different stacking modes cf.: E. Conwell, *Semiconductors and Semimetals*, vol. 1, Academic Press, New York, **1966**.
[12] G. J. Ashwell, S. C. Wallwork, *Acta Crystallogr.* **1979**, *B35*, 1648−1651.
[13] T. Sundaresan, S. C. Wallwork, *Acta Crystallogr.* **1972**, *B28*, 491−497.
[14] J. P. Pouget in *Organic Superconductors* (Eds.: J. M. Williams, J. R. Ferraro, R. J. Thorn, K. D. Carlson, R. Geiser, H. H. Wang, A. M. Kini, M.-H.Whangbo), Prentice Hall, New Jersey, **1992**, pp. 89−91.
[15] U. Geiser, H. H. Wang, S. M. Budz, M. J. Lowry, J. M. Williams, J. Ren, M. H. Whangbo, *Inorg. Chem.* **1990**, *29*, 1611−1614.
[16] A. P. Phillips, J. Mentha, *J. Am. Chem. Soc.* **1955**, *77*, 6393−6398.
[17] A. P.Gray, T. B. O′Dell, *Nature* **1958**, *181*, 634−635.
[18] R. F. Homer, T. E. Tomlinson, *J. Chem. Soc.* **1960**, 2498−2503.
[19] S. Hünig, D. Scheutzow, H. Schlaf, A. Schott, *Liebigs Ann. Chem.* **1974**, 1423−1435.
[20] A. Aumüller, S. Hünig, *Justus Liebigs Ann. Chem.* **1986**, 142−164.
[21] A. Aumüller, P. Erk, S. Hünig, H. Meixner, J. U. von Schütz, H.-P. Werner, *Liebigs Ann. Chem.* **1987**, 997−1006.
[22] Further details of the crystal-structure investigations are available from CCDC, 12 Union Road, Cambridge CB2 1 EZ, U.K. [Fax: (internat.) + 44(1223)336-033; E-mail: deposit@ccdc.cam.ac.uk], on quoting the depository number CCDC-100795.

[97364]